Semiconductor Physics, Quantum Electronics & Optoelectronics, 2024. V. 27, No 1. P. 054-063.

Semiconductor physics

Effect of annealing in air on the properties of carbon-rich amorphous silicon carbide films

A.M. Lukianov[1,2], M.G. Dusheiko[1,3], V.B. Lozinskii[1,2], V.P. Temchenko[2], V.N. Dikusha[2], N.I. Klyui[1,2]

[1]*College of Physics, Jilin University, 2699 Qianjin Str., Changchun 130012, People's Republic of China*
[2]*V. Lashkaryov Institute of Semiconductor Physics, National Academy of Sciences of Ukraine, 41, prosp. Nauky, 03680 Kyiv, Ukraine*
[3]*National Technical University of Ukraine "Igor Sikorsky Kyiv Polytechnic Institute", 16, Politekhnichna str., 03056 Kyiv, Ukraine*
Corresponding author e-mail: lukyanov_a@ukr.net

Abstract. Thermal stability of thin carbon-rich Si carbide films was studied. Air anneals at the temperatures up to 700 °C were used to model the operation thermal conditions of the films in photoelectronic devices such as solar cells covered by Si carbide antireflection coatings. Si carbide films with different carbon-to-silicon ratios were studied. Annealing in air was shown to lead to consecutive film oxidation and transformation from Si carbides to oxidized Si carbide composites. The oxidized composites demonstrated the changes in thickness, element composition and optical properties as compared to the non-annealed films. At this, the films with higher Si content showed better stability of the optical properties at increased temperatures. During annealing, the increase of the film thickness by Si oxide formation competed with the thickness decrease by formation and evaporation of carbon oxide.

Keywords: amorphous Si carbide films, PECVD, annealing.

https://doi.org/10.15407/spqeo27.01.054
PACS 78.20.-e, 78.30.Ly, 81.16.Pr, 81.40.Ef

Manuscript received 15.11.23; revised version received 10.01.24; accepted for publication 28.02.24; published online 12.03.24.

1. Introduction

Thermal stability of antireflection and protective coatings for solar cells is the one of key issues of their successful implementation in devices. Amorphous Si and Si carbide films are widely used as such coatings for Si solar cells. The thermal properties of such films were studied in a number of works. However, additional study of their thermal stability in air ambient is still required.

Anneals in a neutral ambient or in vacuum are widely used to form nanoscale structures [1–3]. In [4], amorphous hydrogenated Si carbide films (a-SiC_x:H) were annealed in argon protective environment for 30 min at different temperatures. The researchers observed formation of amorphous carbon nanodots within the a-SiC_x:H films after annealing at the temperatures of 600 °C and higher. At higher temperatures, near-surface film oxidation became strong. It was shown from the analysis of the film absorption spectra that the decrease of the optical band gap can be attributed to the formation and graphitization of the carbon nanodots within the a-SiCH films.

The as-deposited samples were subsequently annealed at the temperatures of 900 °C and 1000 °C in nitrogen ambient. Formation of nanocrystalline Si (ncSi) dots in the amorphous Si carbide (a-SiC) host matrix after 1 h anneals was demonstrated [5].

It was found in [6] that the oxidation properties of a-Si-C-N:H films were mainly due to the formation of Si dangling bonds and smaller carbon nanoclusters.

Oxidation is a critical issue for Si carbide films subjected to annealing in air. As was shown in [7], the oxidized films demonstrated a continuous increase in the film thickness. This increase was related to the formation of Si oxide from elemental Si. It was accompanied by the competitive thickness decrease due to consumption and evaporation of excess carbon in form of CO. At the same time, the optical absorption edge of the films was found to increase with the annealing temperature. The films annealed in argon and nitrogen ambient under identical conditions did not reveal any shifts in the absorption edge. The observed decrease in the band gap with the annealing temperature was attributed to effusion of hydrogen during annealing and formation of dangling

Table 1. Parameters of the film deposition process.

Sample	*P*, Pa	SiH_4, sccm	Ar, sccm	H_2, sccm	CH_4, sccm	RF, W	*T*, °C	*d*, nm/min
1	50	10	80	120	20	150	200	16.7
2		10				200		20.9
3		10				300		25.7
4		20				150		18.4
5		20				200		24.7
6		20				300		34.9

bonds and microvoids. Moreover, a blue shift of the band edge was observed that might be interpreted as being due to the formation of SiC nanoclusters surrounded by SiO_2 or the homogeneous alloying of amorphous SiC and SiO_2. As the amorphous films were annealed in oxygen ambient, they gradually became a mixture of amorphous SiC and SiO_2. Such structural changes caused an increase in the band gap as more SiO_2 was formed. The calculated ratio of the oxygen concentration in SiC was in a good agreement with the band gap energies derived from the absorption studies.

It was shown that more carbonized films formed more sp^3 carbon bonds that stabilize the structure and graphitized at higher annealing temperatures as compared to pure diamond-like carbide films. The observed oxidation takes place at the temperatures above 300 °C. Pure diamond-like carbide films even disappear at the temperatures higher than 500 °C. For silicon-doped diamond-like carbide, observable but insignificant oxidation occurs at 300 °C, while the remaining carbon converts to graphite phase at 600 °C.

As annealing of amorphous silicon-carbon films in air leads to the growth of the film thickness, the oxide shows a decreasing trend with temperature indicating that oxidation of SiC films is a diffusion-limited process [8].

In this work, we systematically study amorphous hydrogenated Si carbide (a-SiCH) films subjected to air annealing at the temperatures up to 700 °C by optical UV-visible-near IR, FTIR spectroscopy and EDS composition evaluation.

2. Experimental

a-SiCH films were deposited by PECVD technique using a Sentech Depolab 200 system with capacitively coupled electrodes. The substrates for the deposition were boron-doped CZ Si (100) with the resistivity of 1…5 Ohm·cm, 1 mm thick quartz plates and Al foil. Before loading into the PECVD chamber, the substrates were washed in an ultrasound bath for 5 min in distilled water and absolute ethanol, and dried with compressed nitrogen. The Si substrates were additionally rinsed in HF 5% solution for 15 s to remove natural oxide and then washed with distilled water and dried with compressed nitrogen.

After vacuum pumping, plasma treatments were performed to remove possible organic contaminations from the substrates surfaces. For that, H_2 was introduced into the chamber at the flow rate of 200 sccm and the pressure of 50 Pa. The RF plasma discharge power (DP) was set to 50 W for 5 min. After that, the substrates were heated at the heating rate of 4 °C/min to the process temperature.

The films were deposited from the gas mixture of methane, silane, hydrogen and argon. The gas mixture was controlled by mass-flow controllers. The gas flow rates were: Ar – 80 sccm (standard cubic centimeters per minute), H_2 – 120 sccm, and CH_4 – 20 sccm. It should be noted that SiH_4 in this study was diluted by He to 5% and its flow rate values presented in Table 1 are the values for that mixture. The pressure in the chamber was 50 Pa, the deposition temperature was 200 °C and the DP varied from 100 to 300 W.

After deposition, the samples were naturally cooled down to the room temperature in Ar ambient atmosphere.

Anneals of the samples were carried out in a tube furnace in air ambient. Each sample (on quartz, Al foil and Si substrates) was preliminary characterized and then cut in 4 pieces. Batches of samples on the quartz, Al foil and Si substrates were placed into the furnace tube preheated to the target temperature for 30 min and then removed and naturally cooled down. The annealing temperatures were set to 400, 500, 600 and 700 °C. The anneal at 700 °C was carried out only for the samples on the quartz and Si substrates to avoid contamination of other samples in the batch with Al.

To evaluate the thicknesses and refractive indices, a laser ellipsometer Sentech LE400 with the wavelength λ = 632 nm and the simple single-layer optical model of an amorphous film on a Si substrate were used.

The transparency and reflectance of the obtained films deposited on the Si and quartz substrates were measured by a spectrophotometer Agilent Cary 5000 in the UV-visible near spectral range of 200…1100 nm. Using the obtained spectra, the Tauc curves where calculated. The optical band gap values were estimated from the plotted Tauc curves using the following relationship:

$$(\alpha E)^{1/2} = A(E - E_{opt}),$$

where α is the absorption coefficient, A is the constant, and E_{opt} is the optical band gap value, respectively.

The values of thicknesses and refractive indices of the annealed films were obtained from the laser ellipsometry (LE) measurements.

To evaluate the optical properties in the IR range, a FTIR setup Shimadzu IRAffinity-1S was used with an attenuated total reflection (ATR) accessory. The spectra of the samples deposited on the Al foil were measured to exclude the Si and O parasitic background for the samples grown on the quartz and Si substrates. The dynamics of the changes in atomic bond vibrations as well as the types of atomic bonds for the initial samples and the samples annealed at the temperatures of 400…600 °C were obtained.

A SEM FEI XL-30 was used for additional thickness measurements and microstructure analysis. An EDS accessory X-Max of the Oxford Instruments was used to determine the silicon, oxygen and carbon contents. The Si content was determined as the ratio [Si]/([Si] + [C]) of the element concentrations obtained from the EDS measurements of the films deposited onto the Al foils.

3. Results and discussion

The results of the EDS element analysis of the studied films annealed at different temperatures is presented in Fig. 1 for low-Si content (a) and Si-enriched films (b), as well as in Table 2. As one can see from this figure, in the low-Si content films the carbon content decreases even at low annealing temperature of 300 °C, making the films closer in stoichiometry to pure SiC. At the same time, oxygen content in both film series begins to increase at a much higher temperature (600 °C). The Si-enriched a-SiCH films show better content stability being annealed at the temperatures up to 500 °C. It may be supposed that C leaves the films during annealing. Such behavior can explain the thickness decrease at high temperatures.

Figs. 2 and 3 present the film thicknesses obtained from the LE measurements. It can be seen from this figure that the thicknesses change nonmonotonously with temperature, which confirms carbon evaporation from the samples during annealing. One may conclude from the analysis of the two series of the low-Si content and Si-enriched films deposited at the smaller (20 sccm) and larger (20 sccm) silane flow rates, respectively, that the

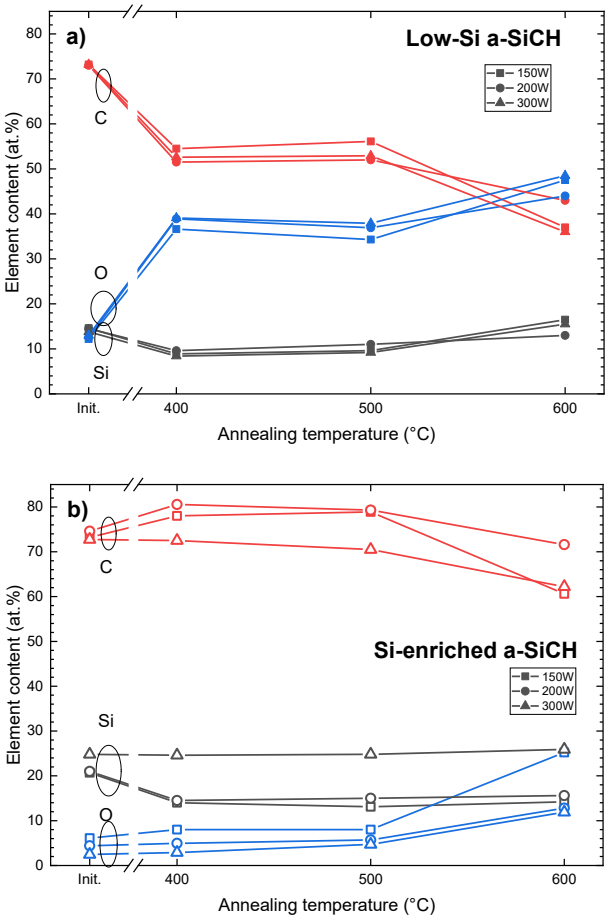

Fig. 1. Effect of annealing temperature on the element content of the films: a) low-Si content a-SiCH films; b) Si-enriched a-SiCH films. Red lines correspond to carbon, blue ones – to silicon and black ones – to oxygen. Symbols correspond to the deposition power: squares – 150 W, circles – 200 W, and triangles – 300 W. (Color online)

former films have lower thermal stability and are easier oxidized at lower temperatures, promoting to the thickness decrease due to carbon evaporation. This finding agrees with [7], where the changes of the thicknesses of Si carbide films during thermal oxidation were observed. At the same time, higher temperatures led to film thinning due to formation of CO and its evaporation.

Table 2. Calculated optical band gap and Si content (from EDS measurements) in the initial films.

Sample	E_{opt}, eV	Si/(Si + C), %
1	3.4	25.8
2	3.25	23.7
3	3.1	22.0
4	3.07	25.7
5	2.9	27.6
6	2.72	28.0

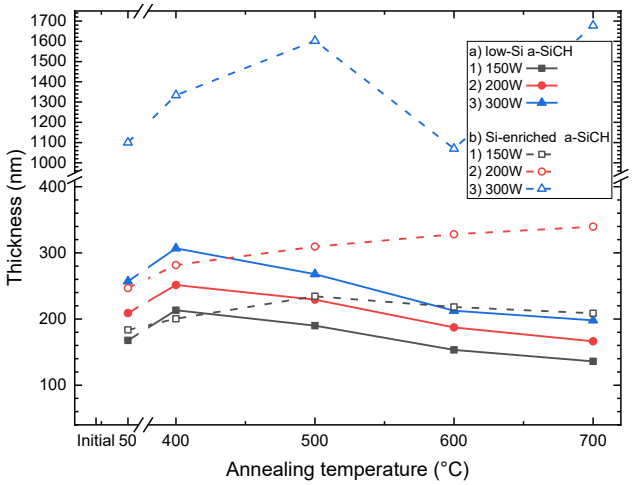

Fig. 2. Effect of annealing temperature on the film thickness: a) low-Si content a-SiCH films; b) Si-enriched a-SiCH. The PECVD plasma power during film deposition: 150 (*1*), 200 (*2*), and 300 W (*3*).

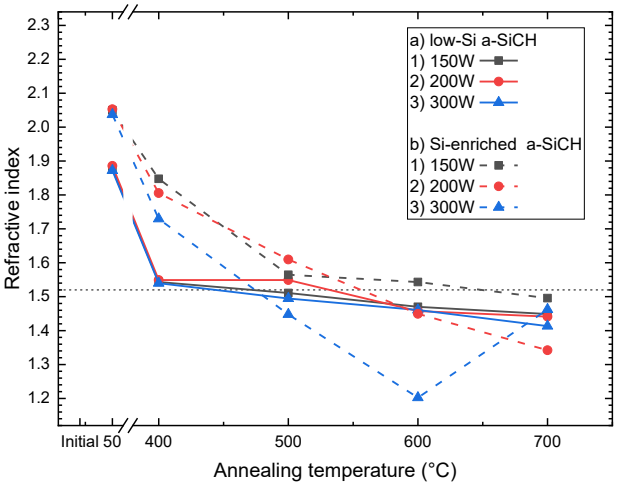

Fig. 4. Effect of annealing temperature on the refractive index at λ = 632 nm for: a) low-Si content a-SiCH films; b) Si-enriched a-SiCH. The PECVD plasma power during film deposition: 150 (*1*), 200 (*2*), and 300 W (*3*).

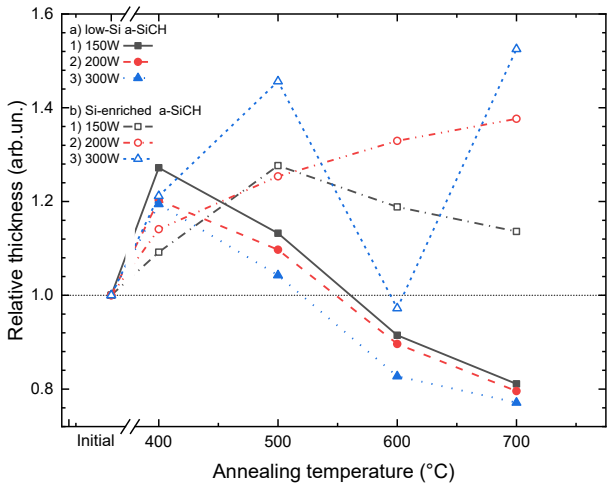

Fig. 3. Effect of annealing temperature on the relative thickness changes of the films: a) low-Si content a-SiCH films; b) Si-enriched a-SiCH. The PECVD plasma power during film deposition: 150 (*1*), 200 (*2*), and 300 W (*3*).

The second series of the Si-enriched films prepared at the higher silane flow rate shows better resistance to thermal changes in thickness. The films oxidation level increased that was reflected by their thickening with annealing temperature due to Si oxidation. It should be noted that the films did not reach the critical oxidation and structure changes that would lead to formation and evaporation of CO species, unlike the first film series. However, the last sample prepared at the high silane flow rate and the highest RF plasma power showed the annealing behavior similar to that of the first series of the films.

The film refractive indices calculated from the reflectance measurements (Fig. 4) show their monotonous decrease with the annealing temperature. The structure and composition of the first group of the samples with the smaller Si content rapidly changed at the temperature of 400 °C leading to the decrease of their refractive index from about 1.88 to 1.55. Anneals at the rest temperatures had almost no effect on the mentioned characteristic, which remained in the range of 1.49…1.44.

The second series of the samples grown at the higher silane flow rate slowly oxidized in the whole range of the annealing temperatures of 400…700 °C, achieving similar values of the refractive index to that of the first series at a sufficiently higher temperature of 600 °C.

The measured reflectance and transparency spectra of the films grown on the quartz substrates allowed to evaluate the film Tauc dependences (Fig. 5) and calculate their optical (Tauc) band gaps as shown in Fig. 6. The structural changes in the films after annealing led to the formation of complex composite structures consisting of silicon and carbon oxides and nanoscale oxidized Si carbide clusters. Such structure was manifested by the bends of the Tauc curves that complicated the evaluation and increased the error of the estimated band gap values.

It should be noted that the values of optical band gaps of the films did not change for the annealing temperatures up to 500 °C. When the annealing temperature was raised above this value, the a-SiCH films with low and higher Si content revealed different behaviors. The films with low Si content showed the increase in the band gap values toward to the values for Si oxide. At the same time, the optical band gap of the films enriched with Si decreased.

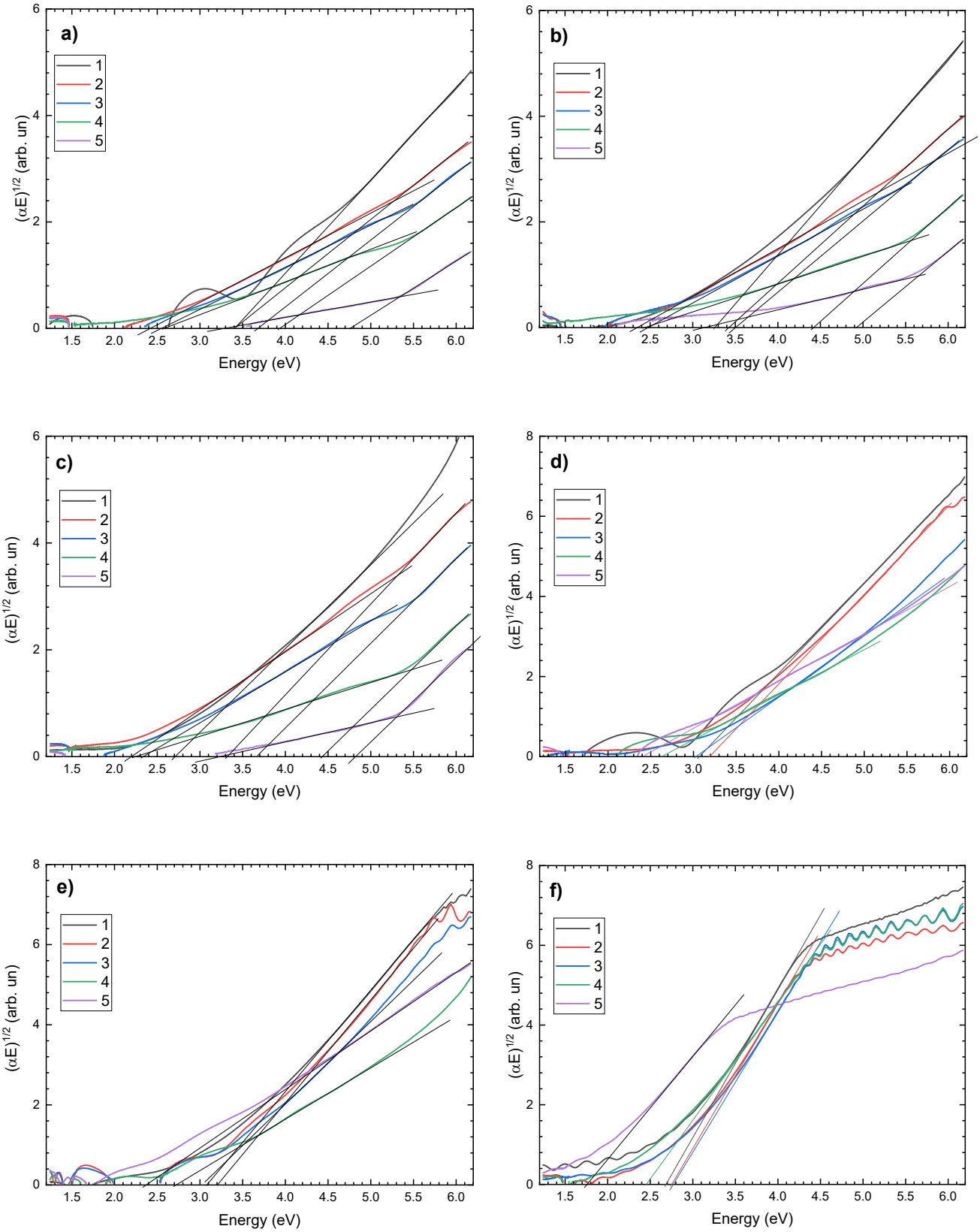

Fig. 5. Tauc curves for the initial and annealed films: low-Si content a-SiCH films deposited at 150 (a), 200 (b), and 300 W (c); Si-enriched a-SiCH films deposited at 150 (d), 200 (e), and 300 W (f); *1* – initial films, *2–5* – films annealed at 400, 500, 600, and 700 °C, respectively.

Table 3. Identification of the positions of the FTIR peaks for the studied a-SiCH films.

No	Approx. peak position, cm^{-1}	Bond type	Reference
1	440	Si–O–Si rocking	[9–13]
2	805	Si–C stretching	[14–17]
3	845.5	H–Si–O, Si–C, CH_3	[18]
4	865	H–SiO_2	[18]
5	890	H–SiO_3	[19]
6	1000	Si=C	[20]
7	1029	Silicon suboxide, Si–O–Si	[19]
8	1050	Si–O–Si asymmetric stretching	[11, 13, 21]
9	1137.5	Si–O–Si, Si–O–C	[19]
10	1180	Si–O	[9, 21]
11	1260	Si–$(CH_3)_x$ deformation	[15, 16, 21, 22]
12	1260	Si–$(CH_3)_x$–O	[20]

As was noted above, the film thicknesses increased after annealing at 400 °C. Such changes are caused due to the incorporation of oxygen into the film structure, replacement of hydrogen with simultaneous growth of the film volume, and evaporation of weakly bonded carbon species from the films. At the same time, higher annealing temperatures led to the stronger interaction of oxygen by "burning" of some amount of the film content and evaporation of the reaction products resulting in the reduction of the film thickness.

In the case of the low-Si content films deposited at the silane flow rate of 10 sccm, the higher annealing temperatures led to the increase of their optical band gap. It can be explained by preferential breaking of the bonds of sp^2-hybridized C atoms in the films and atom evaporation. As a result, the films with low Si content transformed after annealing to the structure with a larger amount of sp^3-C atoms and, consequently, higher E_{opt}.

At the same time, the Si-enriched films obtained at the silane flow rate of 20 sccm showed the behavior opposite to that described above. This allows us to conclude that amount of Si in carbon films is a critical parameter determining not only the structure of the initial a-SiCH films but also their resistance to the harsh environmental conditions such as high temperatures.

Analysis of the FTIR spectra (Fig. 7, Table 3) shows that the mentioned behavior is related to the formation of Si–O bonds by preferential Si oxidation. Hence, the annealed films transform from Si carbide to Si oxicarbides. It should be noted that after annealing the Si-enriched a-SiCH films show an increase of the intensities of the peaks at 1100…1300 cm^{-1} corresponding to Si–O, Si–O–C and Si–$(CH_3)_x$ bonds.

This reflects structural deformations due to oxygen incorporation into the films. The resolution of the FTIR spectra allowed detecting the presence of typical peaks in the range of 2800…3000 cm^{-1} corresponding to C–H bonds. However, this resolution was not sufficient to analyze correctly the behavior of these peaks during annealing.

It should be noted that the FTIR peaks obtained with the ATR accessory can be shifted with respect to the conventional FTIR peaks obtained in transmittance or reflectance mode. However, the proposed peak assignments are in a good agreement with reference data.

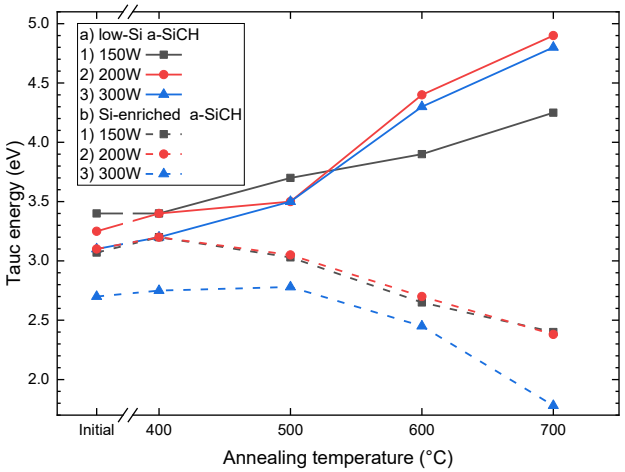

Fig. 6. Effect of annealing temperature on optical (Tauc) band gap of the films: a) low-Si content a-SiCH films; b) Si-enriched a-SiCH films; *1–3* – films deposited at the RF plasma power of 150, 200, and 300 W, respectively.

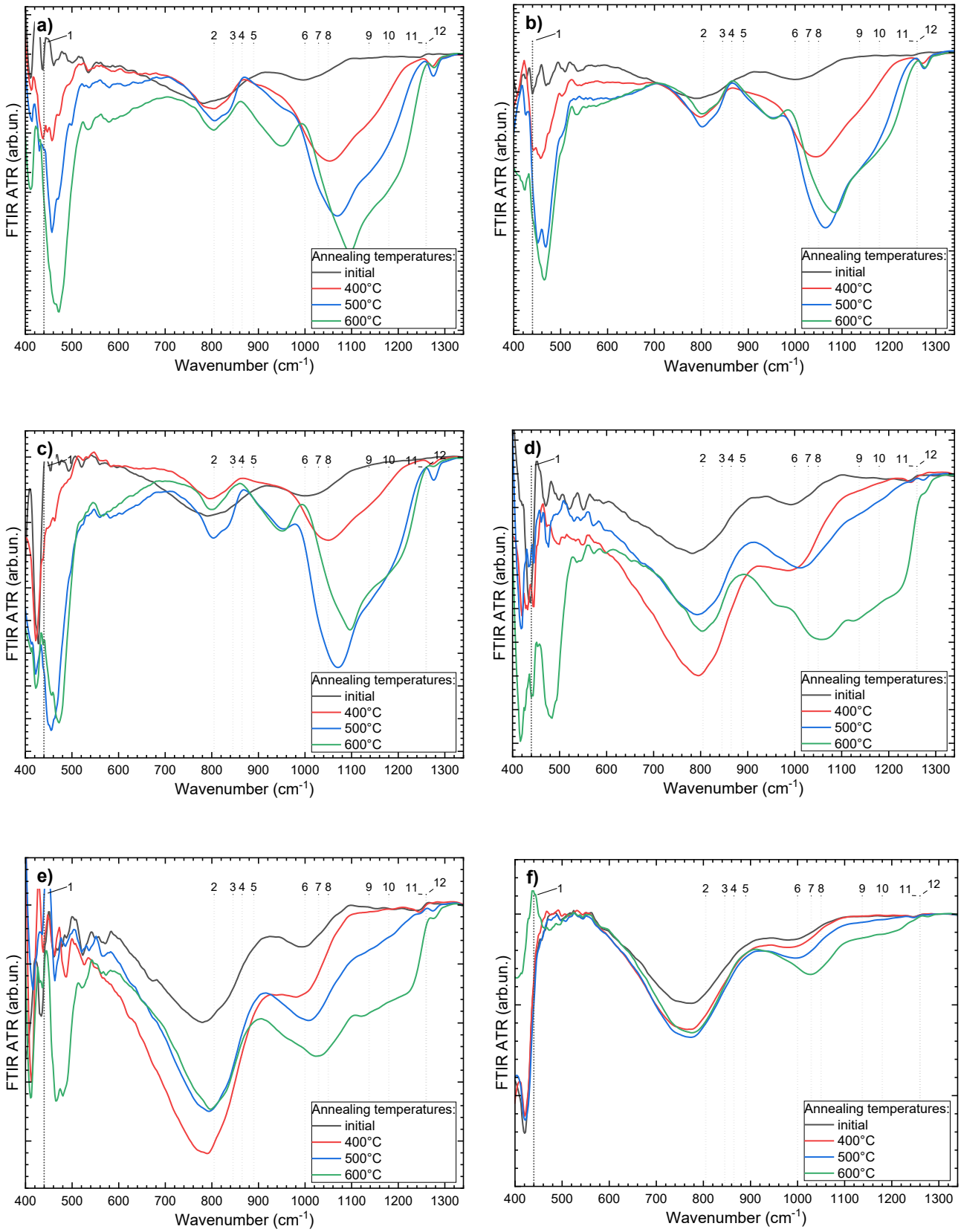

Fig. 7. Effect of annealing temperature on FTIR spectra of the initial and annealed films (peak referenced in Table 3): low-Si content a-SiCH films deposited at 150 (a), 200 (b), and 300 W (c); Si-enriched a-SiCH films deposited at 150 (d), 200 (e), and 300 W (f); black lines – initial films, red, blue, and green lines – the films annealed at 400, 500, and 600 °C, respectively. (Color online)

4. Conclusions

The behavior of the two series of the low-Si content and Si-enriched a-SiCH films deposited by PECVD after annealing in air at the temperatures of 400…700 °C was studied.

It was shown that annealing in air led to consecutive oxidation with complex transformation of the films from Si carbide to oxidized Si carbide composites accompanied by the changes in the film thickness and element composition. The films with the higher Si content showed better stability of the optical properties at the increased temperatures. During annealing, film thickening by Si oxide formation competed with evaporation of carbon oxide and thickness decrease.

The oxidation mechanism proposed based on the analysis of the FTIR spectra consists in hydrogen release mainly from the Si–H bonds and its replacement by oxygen species from air.

Acknowledgments

This work was carried out in the framework of the research project “Creation of basic technologies for the formation of semiconductor materials and structures for nano- and optoelectronics (code: III-10-21)” and the NFU project No. 200/0103 “Development of the technology of biocompatible antibacterial coatings for orthopedic implants by the method of gas detonation deposition for the needs of military and civilian medicine”.

References

1. Wen G., Zeng X., Li X. The influence of annealing temperature on the synthesis of silicon quantum dots embedded in hydrogenated amorphous Si-rich silicon carbide matrix. *J. Non-Cryst. Solids*. 2016. **441**. P. 10–15. https://doi.org/10.1016/j.jnoncrysol.2016.03.006.
2. Xue K., Niu L.-S., Shi H.-J., Liu J. Structural relaxation of amorphous silicon carbide thin films in thermal annealing. *Thin Solid Films*. 2008. **516**. P. 3855–3861. https://doi.org/10.1016/j.tsf.2007.06.194.
3. Hong R.D., Chen X.P., Huang Q. *et al.* High temperature annealing amorphous hydrogenated SiC films for the application as window layers in Si-based solar cell. *Appl. Mech. Mater*. 2013. **401-403**. P. 631–634. https://doi.org/10.4028/www.scientific.net/AMM.401-403.631.
4. Jiang L., Peng Y., Wang T. *et al.* The influence of annealing treatments on the microstructural and optical properties of a-SiC_x:H films embedded with carbon nanodots. *J. Alloys Compd*. 2020. **817**. P. 152772. https://doi.org/10.1016/j.jallcom.2019.152772.
5. Li S., Rui Y., Cao Y., Xu J., Chen K. Annealing effect on optical and electronic properties of silicon rich amorphous silicon-carbide films. *Front. Optoelectron*. 2012. **5**, No 1. P. 107–111.
6. Jianga L., Tiana H., Lib J. *et al*. The influence of NH_3 flow rate on the microstructure and oxidation properties of a-Si-C-N:H films prepared by PECVD technology. *Appl. Surf. Sci*. 2020. **513**. P. 145861. https://doi.org/10.1016/j.apsusc.2020.145861.
7. Wu W.-J., Hon M.-H. Thermal stability of diamond-like carbon films with added silicon. *Surf. Coat. Technol*. 1999. **111**. P. 134–140. https://doi.org/10.1016/S0257-8972(98)00719-1.
8. Sundaram K.B., Alizadeh Z., Chow L. The effects of oxidation on the optical properties of amorphous SiC films. *Mater. Sci. Eng. B*. 2002. **90**. P. 47–49. https://doi.org/10.1016/S0921-5107(01)00827-3.
9. Zhang B.R., Yu Z., Collins G.J., Hwang T., Ritchie W.H. Chemical composition of soft vacuum electron beam assisted chemical vapor deposition of silicon nitride/oxynitride films *versus* substrate temperature. *J. Vac. Sci. Technol. A*. 1989. **7**, No 2. P. 176–188. https://doi.org/10.1116/1.575749.
10. Ravi K.V., Koch C.A., Olson D.S. *et al.* Electrical conductivity of combustion flame synthesized diamond. *Appl. Phys. Lett*. 1994. **65**, No 17. P. 2229–2231. https://doi.org/10.1063/1.111685.
11. Kim M.T. Deposition kinetics of silicon dioxide from hexamethyldisilazane and oxygen by PECVD. *Thin Solid Films*. 1999. **347**, No 1–2. P. 99–105. https://doi.org/10.1016/S0040-6090(98)01729-5.
12. Wang Y.H., Moitreyee M.R., Kumar R. *et al.* A comparative study of low dielectric constant barrier layer, etch stop and hardmask films of hydrogenated amorphous Si–(C, O, N). *Thin Solid Films*. 2004. **460**. P. 211–216. https://doi.org/10.1016/j.tsf.2004.01.055.
13. Banerji N., Serra J., Chiussi S. *et al*. Photo-induced deposition and characterization of variable bandgap a-SiN:H alloy films. *Appl. Surf. Sci*. 2000. **268**, No 1–4. P. 52–56. https://doi.org/10.1016/S0169-4332(00)00583-3.
14. Soum-Glaude A., Thomas L., Tomasella E. Amorphous silicon carbide coatings grown by low frequency PACVD: Structural and mechanical description. *Surf. Coat. Technol*. 2006. **200**, No 22–23. P. 6425–6429. https://doi.org/10.1016/j.surfcoat.2005.11.066.
15. Thomas L., Maille L., Badie J.M., Ducarroir M. Microwave plasma chemical vapour deposition of tetramethylsilane: Correlations between optical emission spectroscopy and film characteristics. *Surf. Coat. Technol*. 2001. **142**, No 9. P. 314–320. https://doi.org/10.1016/S0257-8972(01)01081-7.
16. Di Mundo R., d’Agostino R., Fracassi F., Palumbo F. A novel organosilicon source for low temperature plasma deposition of silicon nitride-like thin films. *Plasma Process. Polym*. 2005. **2**, No 8. P. 612–617. https://doi.org/10.1002/ppap.200500035.
17. Wrobel A.M., Wickramanayaka S., Kitamura K. *et al*. Structure-property relationships of amorphous hydrogenated silicon-carbon films produced by atomic hydrogen-induced CVD from a single-source precursor. *Chem. Vap. Deposition*. 2000. **6**, No 6. P. 315–322. https://doi.org/10.1002/1521-3862(200011)6:6<315::AID-CVDE315>3.0.CO;2-7.

18. Bulou S., Brizoual L., Miska P. *et al*. The influence of CH_4 addition on composition, structure and optical characteristics of SiCN thin films deposited in a CH_4/N_2/Ar/hexamethyldisilazane microwave plasma. *Thin Solid Films*. 2011. **520**, No 1. P. 245–250. https://doi.org/10.1016/j.tsf.2011.07.054.
19. Grill A., Neumayer D.A. Structure of low dielectric constant to extreme low dielectric constant SiCOH films: Fourier transform infrared spectroscopy characterization. *J. Appl. Phys*. 2003. **94**, No 10. P. 6697–6707. https://doi.org/10.1063/1.1618358.
20. Launer P.J., Arkles B. (Eds.). Infrared Analysis of Organosilicon Compounds: Spectra-Structure Correlations. In book: *Silicon Compounds: Silanes & Silicones*. Gelest, Inc Morrisville, PA, 2013. P. 175–178.
21. Banerji N., Serra J., Gonzalez P. *et al*. Oxidation processes in hydrogenated amorphous silicon nitride films deposited by ArF laser-induced CVD at low temperatures. *Thin Solid Films*. 1998. **317**, No 1–2. P. 214–218. https://doi.org/10.1016/S0040-6090(97)00621-4.
22. Blaszczyk-Lezak I., Wrobel A.M., Aoki T. *et al*. Remote nitrogen microwave plasma chemical vapor deposition from a tetramethyldisilazane precursor. 1. Growth mechanism, structure, and surface morphology of silicon carbonitride films. *Thin Solid Films*. 2006. **497**, No 1–2. P. 24–34. https://doi.org/10.1016/j.tsf.2005.09.192.

Authors' contributions

Lukianov A.N.: formal analysis, investigation, data curation, visualization, writing – original draft.
Dusheiko M.G.: conceptualization, investigation, writing – review & editing.
Lozinskii V.B.: investigation, resources, methodology, project administration, writing – review & editing.
Temchenko V.P.: writing – review & editing.
Dikusha V.N.: writing – review & editing.
Klyui N.I.: conceptualization, methodology, validation, formal analysis, investigation, data curation, funding acquisition, supervision, writing – original draft.

Authors and CV

Anatolii M. Lukianov, PhD in Solid State Physics, Researcher at the V. Lashkaryov Institute of Semiconductor Physics, NAS of Ukraine. Author of more than 20 publications. Research interests: development of Si solar cells, amorphous silicon and carbon films grown by PECVD technique and their applications for photoelectrical devices to improve their efficiency. https://orcid.org/0000-0001-9321-1891

Mykhailo G. Dusheiko, Leading Engineer of the Research Laboratory of Semiconductor Converters, Department of Microelectronics, Faculty of Electronics at the NTUU "Igor Sikorsky Kyiv Polytechnic Institute". Author of more than 50 publications. Research interests: thin films and thin-film technology of silicon and oxide semiconductors for sensors and solar power converters, solar cell technologies for space and terrestrial applications, technologies for improving the efficiency and degradation resistance of the elements for space applications, sensors.
E-mail: mgd61@ukr.net,
https://orcid.org/0000-0003-2267-6637

Volodymyr B. Lozinskii, PhD in Technical Sciences, Senior Researcher at the V. Lashkaryov Institute of Semiconductor Physics, NASU. Author of more than 30 publications. Research interests: thin-film and coating technologies, effect of various treatments on the properties of semiconductor materials and dielectric films, technologies for improving the optical properties and degradation stability of IR optic elements, photoelectric characteristics of solar cells, coating technologies for medical applications. E-mail: lvb60@ukr.net,
https://orcid.org/0000-0002-7787-0456

Volodymyr P. Temchenko, PhD in Technical Sciences, Senior Researcher at the V. Lashkaryov Institute of Semiconductor Physics, NASU. Author of more than 50 publications. Research interests: modernization of equipment for depositing diamond-like films and semiconductor and ceramic materials layers, development of ceramic coating technologies for medical purposes by the gas detonation deposition method, film formation mechanisms, dependence of the properties of coatings and dielectric and semiconductor materials layers on the technological conditions of production and modification. E-mail: temvp@ukr.net, https://orcid.org/0009-0007-4373-0838

Valeriy N. Dikusha, Junior Researcher at the V. Lashkaryov Institute of Semiconductor Physics, NASU. Research interests: automation of equipment for plasma chemical and gas detonation deposition of functional layers, development of diamond-like carbon film technologies for semiconductor solar energy, IR optical properties of materials and structures, modeling optical properties of multilayer emitting structures. E-mail: axionit@ukr.net,
https://orcid.org/0009-0003-0965-9952

Nikolai I. Klyui

06.10.1959 – 17.03.2022

Doctor of Sciences in Physics and Mathematics, Professor, Head of Laboratory at the V. Lashkaryov Institute of Semiconductor Physics, NAS of Ukraine. Winner of the State Prize of Ukraine in Science and Technology, 2012. Author of more than 160 publications. Research interests: thin-film and coating technologies, optical and mechanical properties of semiconductor and dielectric films, coatings and multilayer structures, solar cells and modules, energy saving devices (lithium/sodium based batteries and supercapacitors), sensors, coating technologies for medical applications.
https://orcid.org/0000-0002-8974-5222

Вплив відпалу на повітрі на властивості плівок аморфного карбіду кремнію, збагаченого вуглецем

А.М. Лук'янов, М.Г. Душейко, В.Б. Лозінський, В.П. Темченко, В.Н. Дікуша, Н.І. Клюй

Анотація. У роботі досліджено стабільність тонких плівок аморфного карбіду кремнію, збагаченого вуглецем, під впливом відпалів. Низькотемпературні відпали на повітрі при температурах до 700 °C було використано для моделювання робочих температурних умов для плівок у таких фотоелектронних пристроях, як сонячні елементи з просвітлюючими покриттями з карбіду кремнію. Досліджено плівки карбіду кремнію з різними співвідношеннями вуглець-кремній. Показано, що відпал на повітрі приводить до послідовного окиснення плівок карбіду кремнію з трансформацією в оксидні кремній-карбідні композити. Товщина, склад та оптичні властивості оксидних композитів змінювалися порівняно з відповідними характеристиками невідпалених плівок. При цьому плівки з більшим вмістом кремнію продемонстрували кращу стабільність оптичних властивостей при підвищених температурах. Під час відпалу збільшення товщини плівок унаслідок утворення оксиду кремнію конкурувало із процесом зменшення товщини завдяки утворенню та випаровуванню оксиду вуглецю.

Ключові слова: плівки аморфного карбіду кремнію, PECVD, відпал.